Torque ripples reduction and speed control of a switched reluctance motor based on artificial intelligence techniques

Rady Farouk Soliman, Mahmoud Ramadan Ahmed, Soliman Mabrouk Sharaf
Department of Electrical Power and Machine Engineering, Faculty of Engineering, Helwan University, Cairo, Egypt

Article Info

ABSTRACT

This paper proposes a technique for reducing torque ripples and speed control of switched reluctance motor (SRM) using artificial intelligence. The controller of SRM is developed based on a fuzzy logic controller using MATLAB/Simulink software. Fuzzy logic controller overcomes the nonlinearity and uncertainty of the SRM. The proposed controller is used for predicting torque ripples and speed control profiles. The machine performance using the proposed controller is compared with using a traditional PI controller. In addition, comparison of motor performance with and without the use of proposed controllers is highlighted. The motor performance is evaluated using the suggested different controllers. The simulation results show that the proposed method indicates a 65% to 75% reduction in torque ripples compared to the traditional PI method.

Corresponding Author:

Rady Farouk Soliman
Department of Electrical Power and Machine Engineering, Faculty of Engineering, Helwan University
Cairo, Egypt
Email: rady.farouk@icloud.com

1. INTRODUCTION

During recent years, switched reluctance motors (SRM) have attracted wide attention because of their simple structure and robustness, which make them economical and suitable for variable-speed drive applications [1]. Without either a commutator or permanent magnets, the SRM structure allows it to operate in harsh environments, thus making it very attractive for applications related to electric vehicles, aerospace, and renewable energy systems [2]. Their tendency to develop torque ripples is one major drawback of the SRMs, despite these advantages.

The primary sources of torque ripples in SRMs arise from the nonlinear interdependence among rotor position, excitation current, and magnetic flux [3]. The interaction between the salient poles of the stator and rotor leads to fluctuations in output torque, which in turn generate undesirable acoustic noise, vibration, and mechanical stress. These features not only degrade the performance of the motor but also limit its pervasiveness in sensitive applications [3].

The reluctance motor is a type of synchronous machine. Its stator windings are wound as field coils, similar to those in a direct current (DC) motor, while its rotor has no coils or magnets. Figure 1 shows the structure of a switched reluctance motor. While both the stator and rotor are salient poles, the machine is considered a doubly salient machine.

The generated torque in a switched reluctance motor is due to reluctance torque. The rotor aligns itself whenever diametrically opposite stator poles are energized. In a magnetic circuit, the rotor naturally moves toward the position of minimum reluctance upon excitation. When two rotor poles align with two stator poles, another set of rotor poles remains out of alignment with a different set of stator poles. Then these stator poles are energized, bringing the rotor poles into alignment with them [4], [5].

This fundamental operation is illustrated in Figure 2. Figure 2 assumes that the rotor poles r_1 and $r_{1'}$ are aligned with the stator poles c and c''. When a current is applied to phase a in the direction shown in Figure 2(a), a magnetic flux is generated through stator poles a and a' and rotor poles r_2 and r_2', which attracts rotor poles r_2 and r_2' toward stator poles a and a'', respectively. Once alignment is achieved, the current in phase a is switched off, as depicted in Figure 2(b).

Next, the stator winding of phase b is energized, causing r_1 and r_1 to move toward b and b' in a clockwise direction. Similarly, when phase c is activated, r_2 and r_2' align with c and c', respectively. By sequentially switching the stator currents in this manner, the rotor continues to rotate. Conversely, reversing the switching sequence to *acb,* results in the rotor rotating in the opposite direction. Since the rotor movement, and thus the generation of torque and power, is achieved by switching currents into the stator windings based on variations in reluctance, this variable-speed motor is known as a switched reluctance motor.

Neglecting the mutual coupling between phases, the electrical equivalent circuit for a switched reluctance motor can be derived as [5], [6]. The voltage applied to a phase is the sum of the voltage drop across the phase winding and the rate of change of flux linkage, expressed as (1).

$$V = R_s i + \frac{d\lambda(\theta,i)}{dt} \tag{1}$$

Where V: applied voltage to a phase, R_s: winding resistance, and λ: flux linkage per phase, expressed as (2).

$$\lambda = iL(\theta,i) \tag{2}$$

Where L is the inductance dependent on rotor position and current.

The single-phase equivalent circuit of a switched reluctance motor is derived by analyzing the voltage applied to a phase winding. The (3) through (7) provide the mathematical formulation for this circuit.

$$V = R_s i + \frac{d\{L(\theta,i)i\}}{dt} \tag{3}$$

$$V = R_s i + L(\theta,i)\frac{di}{dt} + i\frac{dL(\theta,i)}{dt} \tag{4}$$

$$V = R_s i + L(\theta,i)\frac{di}{dt} + i\frac{d\theta}{dt}\frac{dL(\theta,i)}{d\theta} \tag{5}$$

$$V = R_s i + L(\theta,i)\frac{di}{dt} + iW_m\frac{dL(\theta,i)}{d\theta} \tag{6}$$

$$e = iW_m\frac{dL(\theta,i)}{d\theta} \tag{7}$$

Where *e* represents the induced voltage in the stator winding. Hence, the switched reluctance motor is illustrated in Figure 3.
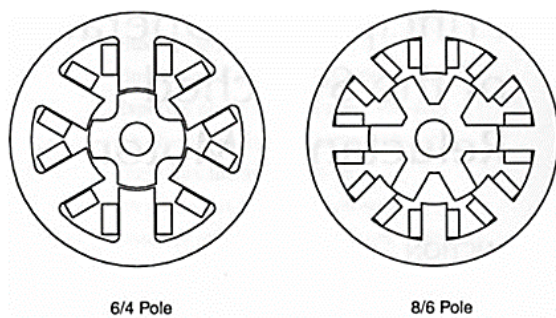

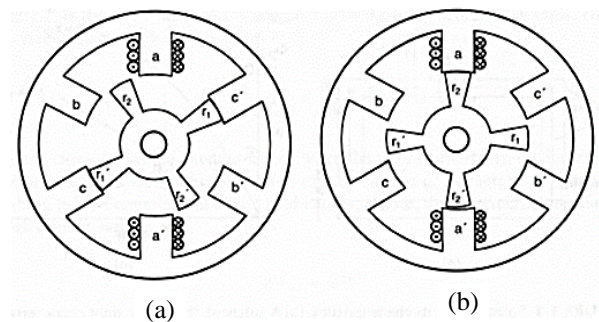Figure 1. Switched reluctance motor configuration

Figure 2. Operation of a switched reluctance motor: (a) alignment of phase C and (b) alignment of phase A

Multiplying (4) by current to get the instantaneous input power to get derivative for electric torque.

$$P = Vi = R_s i^2 + Li(\theta,i)\frac{di}{dt} + i^2\frac{dL(\theta,i)}{dt} \tag{8}$$

$$Li(\theta, i)\frac{di}{dt} = \frac{di}{dt}\left(\frac{1}{2}L(\theta,i)i^2\right) - \frac{1}{2}i^2\frac{dL(\theta,i)}{dt} \tag{9}$$

By substituting (9) into (8), the expression for the instantaneous electromagnetic torque can be derived as shown in (10).

$$P = R_s i^2 + \frac{di}{dt}\left(\frac{1}{2}L(\theta,i)i^2\right) + \frac{1}{2}i^2\frac{dL(\theta,i)}{dt} \tag{10}$$

Where $R_s\ i^2$ represents copper losses, $\frac{di}{dt}\left(\frac{1}{2}L(\theta,i)i^2\right)$ represents the rate of change of field energy, and $\frac{1}{2}i^2\frac{dL(\theta,i)}{dt}$ represents the air gap power P_g.

$$t = \frac{\theta}{W_m} \tag{11}$$

By substituting time in terms of rotor position and rotational speed.

$$P_g = \frac{1}{2}i^2\frac{dL(\theta,i)}{d\theta}\frac{d\theta}{dt} = \frac{1}{2}i^2\frac{dL(\theta,i)}{d\theta}W_m \tag{12}$$

The air gap power, P_g is the product of the electromagnetic torque and rotor speed.

$$P_g = T_e W_m \tag{13}$$

$$T_e = \frac{1}{2}i^2\frac{dL(\theta,i)}{d\theta} \tag{14}$$

Due to the saliency of both the stator and rotor in an SRM, torque ripples are generated during the commutation of one phase and the excitation of the next phase. The point of intersection between the two excited phases contains the torque ripple [7], shown in Figure 4 for a certain motor operation.

The high level of torque ripples in SRMs poses a challenge to the engineers as it has a direct influence on smoothness and efficiency during the operation of the motor. The performance and reliability of the motor can be improved further, mainly in those applications that require precision and stability. Traditional control approaches have been applied to overcome this problem [8]. However, most of these methods fail to cope with the inherent nonlinearities of SRM and their dynamic response under different load conditions, as in [3]. To reduce torque ripples, many papers have reported indirect torque ripples minimization by current compensation profile [9]-[15]. Also, more advanced control techniques have discussed the problem of torque ripples of SRM, offering different solutions [16]-[21].
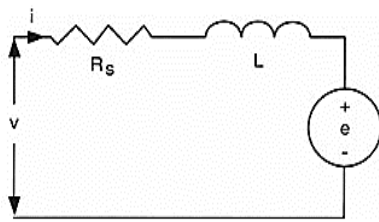

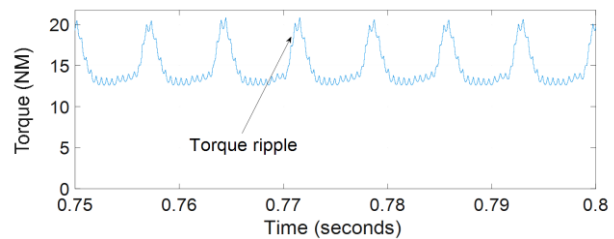Figure 3. The single-phase equivalent circuit of a switched reluctance motor

Figure 4. Torque ripples of SRM

In this paper, a new control based on fuzzy logic control is proposed to reduce torque ripples and enhance speed regulation in SRMs. A fuzzy logic controller is particularly effective in dealing with nonlinear systems, while it can adapt to cope with uncertainty in the system and smoothens the control actions. In this respect, the proposed control approach directly regulates the torque profile by comparing real torque with the reference torque and compensates for any deviation. In this paper, the use of fuzzy logic controller (FLC) in an SRM control system will try to achieve a much bigger reduction of torque ripples compared to traditional PI controllers. The performance of the proposed system is evaluated through simulations, where results will be compared with both PI control and traditional SRM operation without torque compensation.

2. METHOD

2.1. Simulation setup

To ensure reproducibility and provide a clear understanding of the methodology, a detailed description of the simulation setup is added below. The simulation was conducted using MATLAB/Simulink, and the following tools and parameters were employed. The simulation was designed to emulate the operation of a switched reluctance motor under varying conditions. MATLAB/Simulink R2023a was utilized, incorporating the following key components:

- Controllers: i) fuzzy logic controller and ii) proportional-integral (PI) controller.
- Motor model: switched reluctance motor with six stator poles and four rotor poles.
- Hysteresis band current controller: maintains phase currents within a specified range to reduce torque ripples.

The general structure of the simulation is illustrated in Figure 5. The diagram includes the SRM model, torque controller, speed controller, and current controller. These components are interconnected to form a closed-loop system ensuring precise torque ripple reduction and speed regulation.

2.2. Fuzzy logic speed controller

The reference speed input fed to the speed controller is to be followed by the motor speed. In this work, a fuzzy logic speed controller is designed which provides an appropriate reference torque signal in order to regulate the motor speed by taking the speed error as an input. Figure 6 depicts the structure of the fuzzy logic speed controller.

The inputs to the fuzzy logic controller are: speed error (e = reference speed− actual speed), change in speed error (Δe). The output is the reference torque, adjusting the torque of the motor to maintain the set speed. The controller used here enhances precision by the following scaling factors: $G_{es} = 3$, $Gd_{es} = 2$, $G_{dus} = 2$.
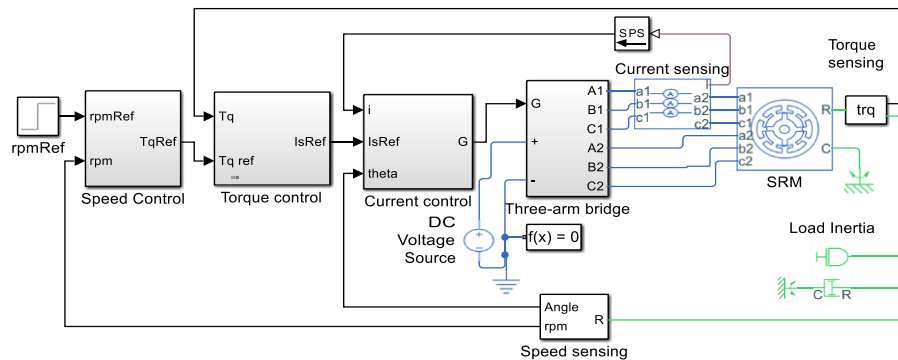

Figure 5. Simulation set up of direct torque control of SRM with torque controller
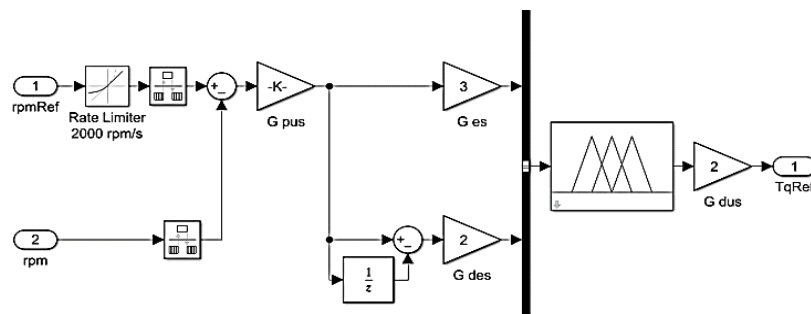

Figure 6. Fuzzy logic speed controller

2.3. Fuzzy logic torque controller

The torque controller compensates for torque ripples by comparing the actual torque with the reference torque and adjusting the motor current accordingly. Figure 7 shows the structure of a fuzzy logic torque controller. The controller calculates the torque error (e = reference torque− actual torque) and change in torque error (Δe). The fuzzy logic system adjusts the reference current signal in such a way as to minimize the torque ripples. The scaling factors for the torque controller are: $G_{et} = 1$, $Gd_{et} = 1$, $G_{dut} = 200$.

2.4. Current controller design

The current controller aims to regulate the current to the SRM such that the actual current follows the reference current profile. This naturally becomes the basis for any torque regulation and ripple reduction. Figure 8 depicts the scheme for current control.

Inputs are the reference signal from the torque controller, phase currents, and rotor position measured by the phase-lock loop (PLL) sensor. The reference current is compared to the measured phase current. This error is then fed into a hysteresis band controller to generate gate signals for the bridge converter. The PLL sensor provides rotor position feedback for the precise control of the commutation angles in the motor. Figure 9 shows the hysteresis current controller.

2.5. Fuzzy logic controller design

The fuzzy controller, as illustrated in Figure 10, consists of components such as fuzzification, an inference mechanism, a rule base, and defuzzification [22], [23]. It regulates the system output based input reference. Both the input and output of the fuzzy controller are crisp values. The fuzzification module converts crisp inputs into fuzzy sets, whereas the defuzzification module translates fuzzy sets back into crisp outputs [24], [25]. The error (e) and the change in error (Δe) are input variables.

$$e(k) = r(k) - y(k) \tag{15}$$

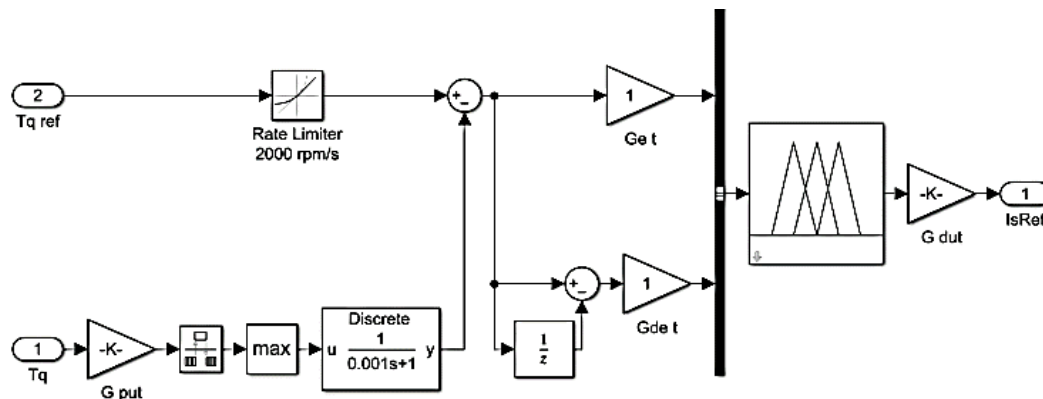$$\Delta e(k) = e(k) - e(k-1) \tag{16}$$
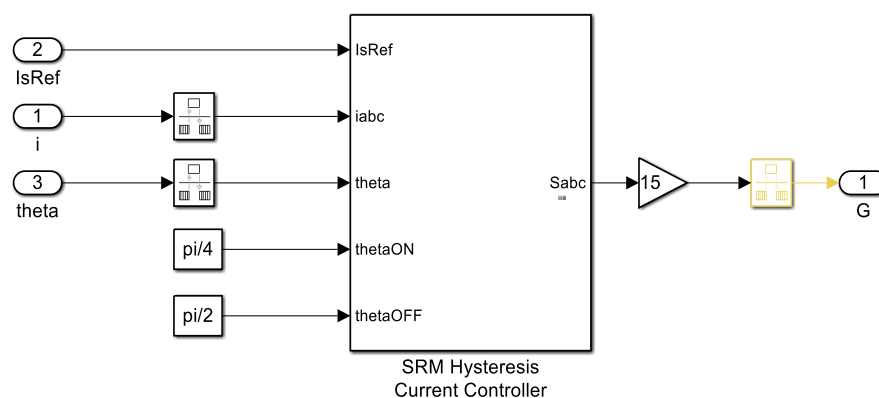

Figure 7. Fuzzy torque controller

Figure 8. Current controller

In this context, r represents the input control signal, while y denotes the system output. The indices k and k−1 correspond to the current and previous states of the system, respectively. The membership functions for the input variables e and Δe, as well as the output variable Δu of the fuzzy controller, are defined based on a 7×7 rule base. These values are normalized within the range [-1.2, 1.2], as shown in Figure 11.

The abbreviations NVB, NB, NM, NS, Z, PS, PM, PB, and PVB correspond to linguistic terms: negative very large, negative large, negative medium, negative small, zero, positive small, positive medium, positive large, and positive very large, respectively. The rule base defines the relationship between the input variables e and Δe and the output variable u. It determines the controller output Δu based on the given inputs e and Δe, as outlined in Table 1.

2.6. System without torque controller

For comparison, a no dedicated torque controller control system was also developed. In that case, the motor is controlled only by a PI speed controller and a current controller, and there is no torque control loop, and hence the torque ripples cannot be suppressed effectively. The block diagram of such a system is given in Figure 12.
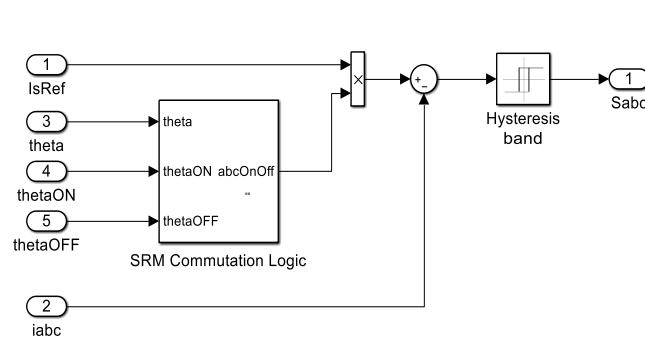

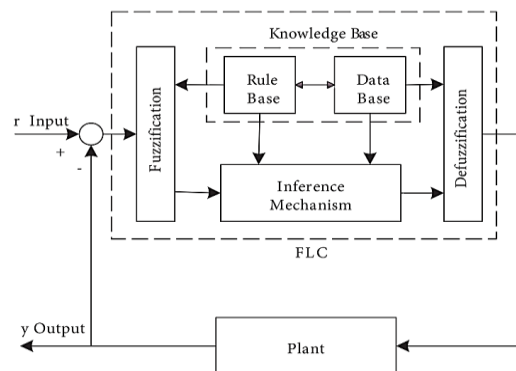
Figure 9. SRM hysteresis current controller

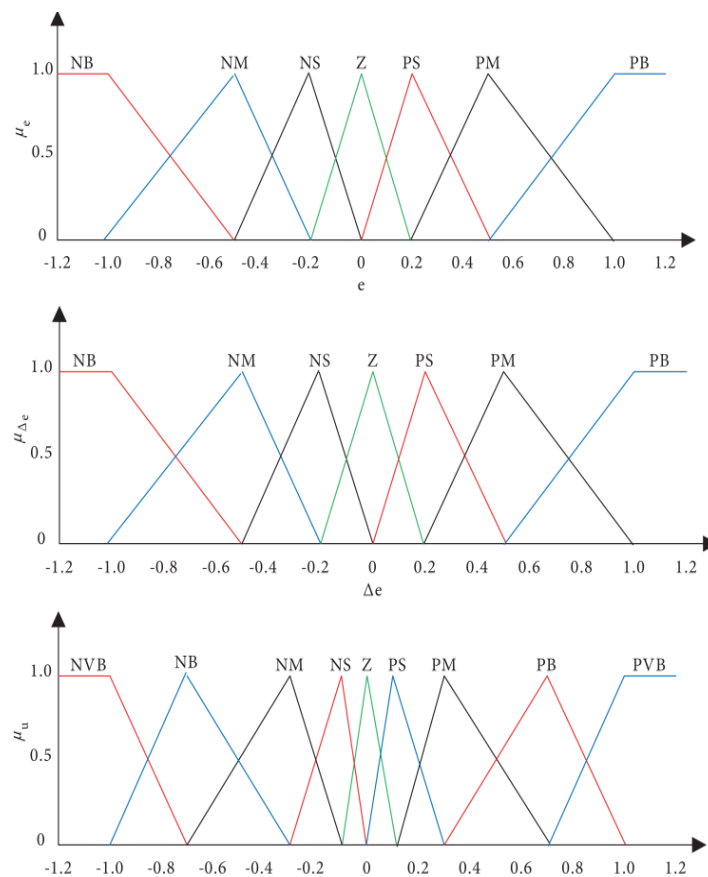Figure 10. Structure of fuzzy logic controller

Figure 11. (7×7) Membership functions

Torque ripples reduction and speed control of a switched reluctance motor based ... (Rady Farouk Soliman)

2.7. Switched reluctance motor parameters

The motor parameters used in the simulation are summarized in Table 2. These values were taken directly from the standard switched reluctance motor model available in MATLAB/Simulink R 2021a. Using this predefined configuration ensures a reliable and validated foundation for simulating the performance of the proposed control strategy.

Table 1. Rule base for output function

Δe ╲ e	NB	NM	NS	Z	PS	PM	PB
NB	NVB	NVB	NVB	NB	NM	NS	Z
NM	NVB	NVB	NB	NM	NS	Z	PS
NS	BVB	NB	NM	NS	Z	PS	PM
Z	NB	NM	NS	Z	PS	PM	PB
PS	NM	NS	Z	PS	PM	PB	PVB
PM	NS	Z	PS	PM	PB	PVB	PVB
PB	Z	PS	PM	PB	PVB	PVB	PVB

Table 2. Motor parameters

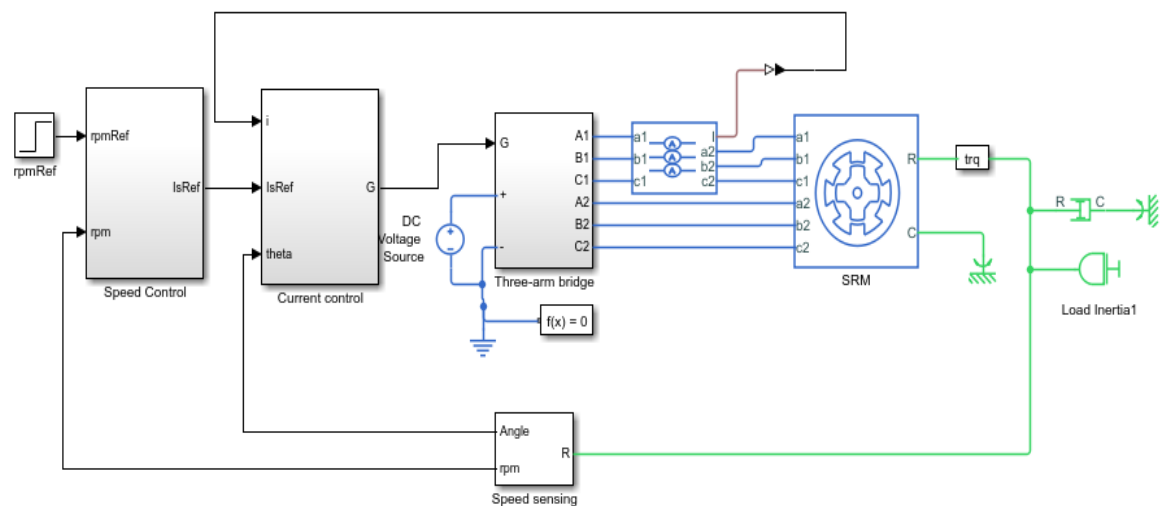| Parameter	Value	Parameter	Value
No of rotor poles	4	Unaligned inductance	6.7e-4 H
No of stator poles	6	DC link voltage	400 V
Stator resistance	3 ohm	Maximum current	180 A
Rotor & load inertia	0.2 Kg·m²	Rotor pole arc	42 degrees
Rotor & load damping	0.2 N·m/ (rad/s)	Stator pole arc	45 degrees
Aligned inductance	0.0046 H	Saturated flux linkage	0.43 Wb

Figure 12. Simulation set up of the control system without a torque controller

3. RESULTS AND DISCUSSION
3.1. Motor performance at 300 RPM

The performance of the motor at 300 RPM is depicted in Figures 13(a) and 13(b), which represent the responses of the speed and torque, respectively, when the system is operating with a fuzzy logic controller, with a PI controller, and without torque control.

3.1.1. Speed response

The fuzzy logic controller reaches the reference speed within approximately 0.22 seconds with a very small percentage overshoot and smooth convergence to 300 RPM as indicated by Figure 13(a). The PI controller takes more time to settle, for which the settling time is approximately 0.3 seconds and overshoots a little. The system without torque control responds very slowly with a great overshoot and a settling time of 0.35 seconds.

3.1.2. Torque response

Figure 13(b) also depicts that the fuzzy logic controller provides an important ripple reduction in torque - the oscillations remain between 6 Nm to 8 Nm. The PI controller reduces torque ripples compared to the system without torque control, but it still maintains wider variations, ripples between 6 Nm and 10 Nm. The system without torque control has the widest ripples that range between 4 Nm and 12 Nm, showing how incompetent it is in controlling the motor torque at 300 RPM.

3.2. Motor performance at 500 RPM

The performance of the motor at 500 RPM is depicted in Figures 14(a) and 14(b). At this speed, the fuzzy logic controller demonstrates faster convergence to the target speed with minimal overshoot, indicating superior dynamic performance. Additionally, the torque ripple remains well-controlled, highlighting the controller's ability to adapt effectively under mid-range speed conditions.
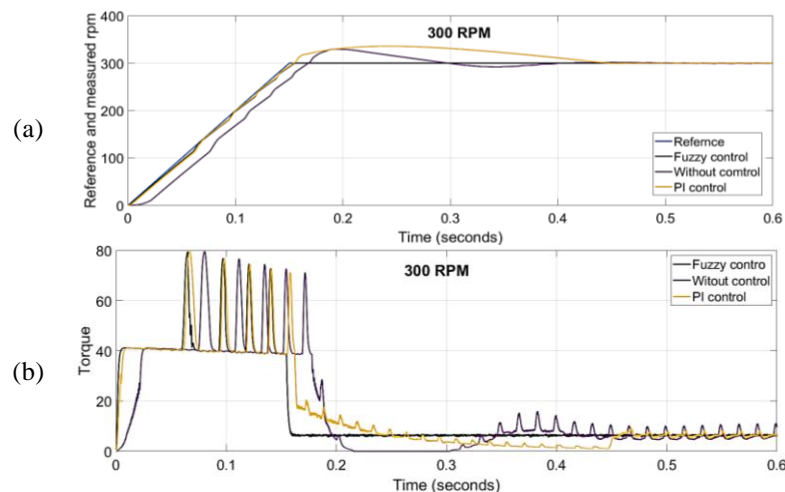

Figure 13. Performance of SRM using fuzzy logic controller and PI controller at 300 rpm: (a) motor speed and (b) motor torque
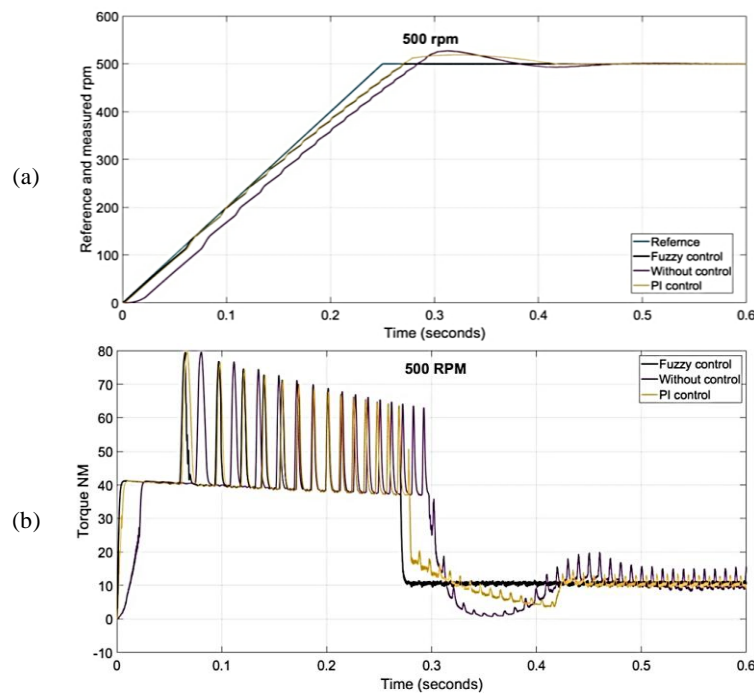

Figure 14. Performance of SRM using fuzzy logic controller and PI controller at 500 rpm: (a) motor speed and (b) motor torque

Torque ripples reduction and speed control of a switched reluctance motor based … (Rady Farouk Soliman)

3.2.1. Speed response

Figure 14(a) depicts that the fuzzy logic controller still remained the fastest response, where the settling has taken place at approximately 0.25 seconds. It provides a much more accurate response by maintaining a very low overshoot. The PI controller is much slower, settling around 0.33 seconds with noticeable overshoot. Whereas, when considering the system without torque control, the overshot is very large and the time for stabilization is higher than 0.35 seconds; thus, the importance of controlling torque in the cause of speed stabilization can be evidenced.

3.2.2. Torque response

Figure 14(b) points out that the fuzzy logic controller performs well in mitigating torque ripples at 500 RPM, maintaining fluctuations between 10 Nm and 12 Nm. The PI controller presents larger torque ripples, oscillating between 10 Nm and 14 Nm. The motor, without torque control, produces the peak quantity of ripples, lying within a range between 9 Nm and 15 Nm, and further shows the inability of the system to suppress torque disturbances appropriately.

3.3. Motor performance at 1000 RPM

The performance at 1000 RPM is demonstrated in Figures 15(a) and 15(b). As the speed increases, the complexity of controlling the SRM also rises due to more pronounced nonlinearities. The fuzzy logic controller still maintains a faster response with lower torque ripple compared to both PI and uncontrolled systems, reaffirming its robustness under high-speed conditions.
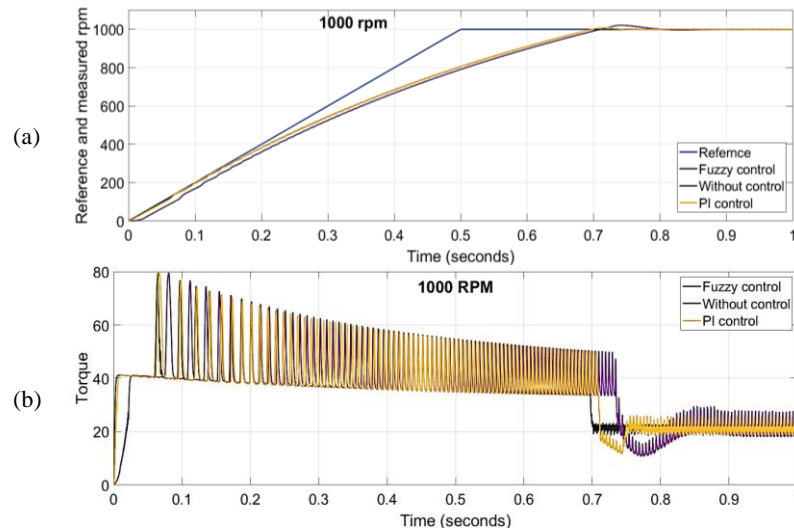

Figure 15. Performance of SRM using fuzzy logic controller and PI controller at 1000 rpm: (a) motor speed and (b) motor torque

3.3.1. Speed response

As seen from Figure 15(a), the fuzzy logic controller maintains its superior adaptability, hence allowing the motor speed to settle down at 0.7 seconds while maintaining the overshoot at the bare minimum. The PI controller is settling down much later at approximately 0.75 seconds with much higher overshoots compared to the fuzzy logic controller. The response is the slowest for the system without torque control, which gets stabilized in more than 0.8 seconds with significant overshoot, indicating an inability of the system to regulate the SRM at high speed.

3.3.2. Torque response

Figure 15(b) shows that the fuzzy logic controller continues its dominance over the PI controller and the system without torque control, keeping the torque ripples in the range from 20 Nm to 24 Nm. The PI controller torque ripples vary within a range of 18 to 26 Nm, which indicates the inability of the PI to cope with higher nonlinearities at 1000 RPM. The maximum torque ripple is for no torque control applied, and it varies between 18 and 30 Nm. In practical applications, this would mean increased mechanical stress and inefficiency.

3.4. Zoomed-in view of torque ripples

Figures 16, 17, and 18 are enlarged torque ripple behaviors for 300 RPM, 500 RPM, and 1000 RPM, respectively, giving further details about the effectiveness of the torque controller in suppressing ripples. These detailed views offer a closer look at the variations across different speed levels and control strategies. They reinforce the claim that the fuzzy logic controller consistently minimizes torque deviations, ensuring more stable and smoother motor operation.

3.4.1. Torque ripples zoom-in view at 300 RPM

Using the fuzzy logic controller, the torque would be smoother and with a few ripples, mostly lying between 6-8 Nm, thus providing more stability during the motor operation. The PI controller produces more ripples, while the oscillations are within 6 Nm and 10 Nm. Ripples are more significant and frequent between 4 Nm and 12 Nm without torque control, which further underlines the incompetence of the system when it comes to dealing with the torque of the motor, as shown in Figure 16.

3.4.2. Torque ripples zoom-in view at 500 RPM

At 500 RPM, the fuzzy logic controller has strict control from 10 Nm to 12 Nm ripples. It proves its effectiveness in the limitation of mechanical perturbations. The PI controller gives the ripples between 10 Nm and 14 Nm, while the most significant ripples are given by the system not under torque control, which also fluctuates between 9 Nm and 15 Nm, as shown in Figure 17.

3.4.3. Torque ripples zoom-in view at 1000 RPM

At 1000 RPM, the fuzzy logic controller again shows its excellence in performance as the ripples remain between 20 Nm to 24 Nm. Larger torque ripples oscillate between 18 Nm and 26 Nm in case of the PI controller, while system without torque control shows the worst performance with ripples from 18 Nm to 30 Nm. This is shown in Figure 18.

3.5. Comprehensive comparison of controllers

Table 3 provides a quantitative comparison of the performance metrics of the fuzzy logic controller, PI controller, and the system without torque control. The comparison is made for different speeds. The performance metrics include settling time and torque ripple amplitude.
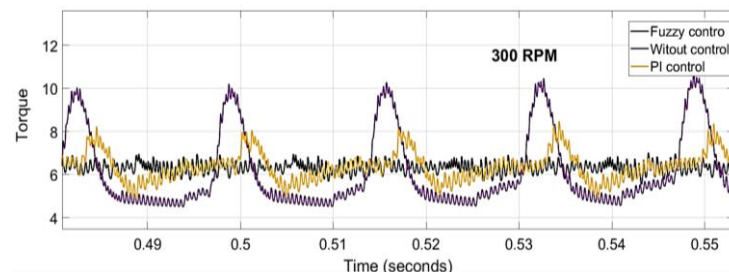

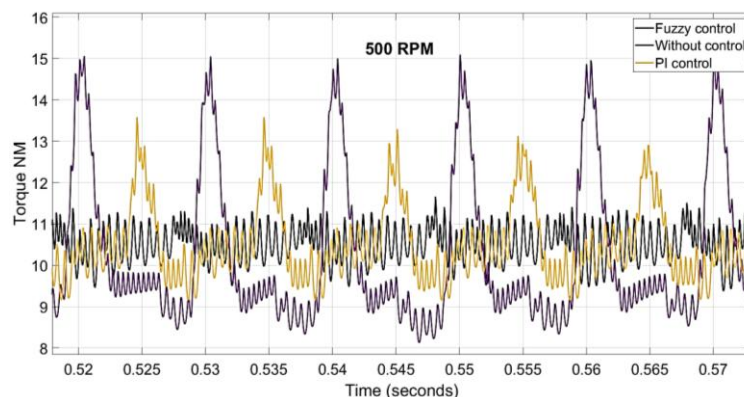Figure 16. Zoom in view of the torque ripples of the SRM at a speed of 300 RPM

Figure 17. Zoom in view of the torque ripples of the SRM at a speed of 500 RPM
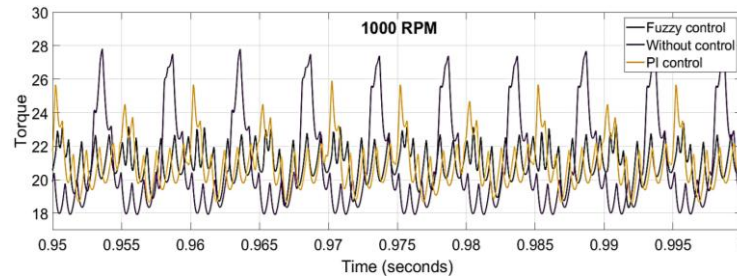
Figure 18. Zoom in view of the torque ripples of the SRM at a speed of 1000 RPM

Table 3. Comparison of performance for different control techniques

Controller	300 RPM	500 RPM	1000 RPM
Fuzzy logic controller	Settling time: 0.22 s	Settling time: 0.25 s	Settling time: 0.7 s
	Torque ripple: 6-8 nm	Torque ripple: 10-12 nm	Torque ripple: 20-24 nm
PI controller	Settling time: 0.3 s	Settling time: 0.33 s	Settling time: 0.75 s
	Torque ripple: 6-10 nm	Torque ripple: 10-14 nm	Torque ripple: 18-26 nm
Without torque control	Settling time: > 0.35 s	Settling time: > 0.35 s	Settling time: > 0.8 s
	Torque ripple: 4-12 nm	Torque ripple: 9-15 nm	Torque ripple: 18-30 nm

3.6. Discussion on the importance of torque control

From the results, one can very clearly understand the underlying significance of having a torque controller fuzzy-based one at that-in an SRM's control scheme:

- Settling time: The fuzzy logic controller provides a much faster and more stable response for all the speeds tested, with a minimum overshoot and steady-state error. Without torque control, poor response creates an overall delay with larger oscillations.
- Torque ripples reduction; The torque ripple is directly compensated by the fuzzy logic controller, and the achieved torque ripples are much smaller compared with that of the PI controller. And even the PI controller presents some improvement compared with the system without torque control, which has very high torque ripples and provides high mechanical stress, resulting in reduced efficiency after time.
- Adaptability: Fuzzy logic controllers are very effective in dealing with the nonlinearities of the SRM, accentuated at high speeds. It is due to this adaptability that the smooth operation of the motor is guaranteed, along with better energy efficiency and reduced wear of the system.

4.   CONCLUSION

A new technique is introduced in this paper for controlling torque ripples of SRMs by incorporating torque control, fuzzy logic, and speed control methods. The novelty in the research work lies in using a dedicated torque controller that dynamically adjusts the magnitude of the torque applied with the explicit aim of minimizing ripples, hence improving the performance characteristics of the motor very significantly. A combination of these controllers provides a robust system that can handle the inherent nonlinearities in SRMs and improve both speed regulation and torque ripple reduction.

The proposed system, implemented with a fuzzy logic controller along with a torque control loop, offers smoother operation of the motor by direct compensation for torque deviations in real time. This leads to lower ripples, especially in the higher speed range, thereby reducing mechanical stresses and acoustic noise. Besides, the control system with fuzzy logic is highly adaptable; it reacts very fast to every change in speed as well as operating conditions. It would ensure faster convergence to the desired speed with a minimum overshoot and steady-state error for speed control.

A combination of a torque controller using fuzzy logic with conventional PI controllers ensures high performance in systems compared to the ones without torque control. The configuration reduces torque ripples while improving general motor efficiency and can be an excellent choice for applications needing high precision, smooth operation, and low noise. These results confirm that the proposed approach represents a considerable contribution to the SRM control strategies for torque ripples reduction and speed regulation improvement.

AUTHOR CONTRIBUTIONS STATEMENT

This journal uses the Contributor Roles Taxonomy (CRediT) to recognize individual author contributions, reduce authorship disputes, and facilitate collaboration.

Name of Author	C	M	So	Va	Fo	I	R	D	O	E	Vi	Su	P	Fu
Rady Farouk Soliman	✓	✓	✓	✓	✓	✓		✓	✓	✓	✓		✓	
Mahmoud Ramadan Ahmed		✓			✓	✓		✓	✓	✓	✓	✓	✓	
Soliman Mabrouk Sharaf	✓		✓	✓			✓			✓	✓		✓	✓

C : **C**onceptualization	I : **I**nvestigation	Vi : **Vi**sualization
M : **M**ethodology	R : **R**esources	Su : **Su**pervision
So : **So**ftware	D : **D**ata Curation	P : **P**roject administration
Va : **Va**lidation	O : Writing - **O**riginal Draft	Fu : **Fu**nding acquisition
Fo : **Fo**rmal analysis	E : Writing - Review & **E**diting	

CONFLICT OF INTEREST STATEMENT

The authors declare that they have no known competing financial interests or personal relationships that could have appeared to influence the work reported in this paper.

DATA AVAILABILITY

The data that support the findings of this study are available from the corresponding author, [RFS], upon reasonable request.

REFERENCES

[1] L. Kalaivani, P. Subburaj, and M. W. Iruthayarajan, "Speed control of switched reluctance motor with torque ripple reduction using non-dominated sorting genetic algorithm (NSGA-II)," *International Journal of Electrical Power & Energy Systems*, vol. 53, pp. 69–77, Dec. 2013, doi: 10.1016/j.ijepes.2013.04.005.

[2] L. Griffin, F. Fleming, and C. S. Edrington, "A particle swarm optimization based maximum torque per ampere control for a switched reluctance motor," in *IECON 2014 - 40th Annual Conference of the IEEE Industrial Electronics Society*, IEEE, Oct. 2014, pp. 343–348. doi: 10.1109/IECON.2014.7048522.

[3] N. Saha, A. K. Panda, and S. Panda, "Speed control with torque ripple reduction of switched reluctance motor by many optimizing liaison technique," *Journal of Electrical Systems and Information Technology*, vol. 5, no. 3, pp. 829–842, Dec. 2018, doi: 10.1016/j.jesit.2016.12.013.

[4] T. J. E. Miller, *Switched reluctance motors and their control*. Oxford: Magna Physics and Clarendon Press, 1993.

[5] R. Krishnan, *Switched reluctance motor drives: Modeling, simulation, analysis, design, and applications*. CRC Press, 2017. doi: 10.1201/9781420041644.

[6] D. A. Shahakar and S. B. Warkad, "An optimal angle control strategy for switched reluctance motor drive in EV applications," *Journal of Control and Decision*, vol. 11, no. 2, pp. 271–282, Apr. 2024, doi: 10.1080/23307706.2022.2150329.

[7] L. Kalaivani, N. S. Marimuthu, and P. Subburaj, "Intelligent control for torque-ripple minimization in switched reluctance motor," in *2011 1st International Conference on Electrical Energy Systems*, IEEE, Jan. 2011, pp. 182–186. doi: 10.1109/ICEES.2011.5725325.

[8] B. E. Azazy, F. E. S. Abdel-Kader, M. Z. Alsherif, and I. M. Abdelqawee, "Improved PI-controller of switched reluctance motor for torque ripple minimization in electric vehicle applications," *Engineering Research Journal (Shoubra)*, vol. 52, no. 1, pp. 171–178, Jan. 2023, doi: 10.21608/erjsh.2022.171006.1104.

[9] Y. Zheng, H. Sun, Y. Dong, and W. Wang, "Torque ripple minimization with current oriented method for switched reluctance motor," *Proceeding of International Conference on Electrical Machines and Systems, ICEMS 2007*, pp. 1640–1644, 2007, doi: 10.1109/ICEMS12746.2007.4412306.

[10] H. Khalili, E. Afjei, and A. Najafi, "Torque ripple minimization in SRM drives using phase/current profiles," in *2007 International Aegean Conference on Electrical Machines and Power Electronics*, IEEE, Sep. 2007, pp. 273–275. doi: 10.1109/ACEMP.2007.4510516.

[11] R. Gobbi and K. Ramar, "Practical current control techniques for torque ripple minimization in SR motors," in *2008 IEEE 2nd International Power and Energy Conference*, IEEE, Dec. 2008, pp. 743–748. doi: 10.1109/PECON.2008.4762573.

[12] I. Husain and M. Ehsani, "Torque ripple minimization in switched reluctance motor drives by PWM current control," *IEEE Transactions on Power Electronics*, vol. 11, no. 1, pp. 83–88, Jan. 1996, doi: 10.1109/63.484420.

[13] J. Mukhopadhyay, S. Choudhury, and S. Sengupta, "ANFIS based speed and current controller for switched reluctance motor," in *2021 IEEE 4th International Conference on Computing, Power and Communication Technologies (GUCON)*, IEEE, Sep. 2021, pp. 1–6. doi: 10.1109/GUCON50781.2021.9573617.

[14] C. Li, C. Zhang, J. Liu, and D. Bian, "A high-performance indirect torque control strategy for switched reluctance motor drives," *Mathematical Problems in Engineering*, vol. 2021, no. 1, p. 6618539, Feb. 2021, doi: 10.1155/2021/6618539.

[15] Z. Tao, M. Li, M. Xu, J. Liu, and J. Luo, "High-precision control for switched reluctance motor with current information," *Frontiers in Energy Research*, vol. 10, p. 894363, Jul. 2022, doi: 10.3389/fenrg.2022.894363.

[16] F. Al-Amyal, L. Számel, and M. Hamouda, "An enhanced direct instantaneous torque control of switched reluctance motor drives using ant colony optimization," *Ain Shams Engineering Journal*, vol. 14, no. 5, p. 101967, May 2023, doi: 10.1016/j.asej.2022.101967.

[17] Z. Xia, G. Fang, D. Xiao, A. Emadi, and B. Bilgin, "An online torque sharing function method involving current dynamics for switched reluctance motor drives," *IEEE Transactions on Transportation Electrification*, vol. 9, no. 1, pp. 534–548, Mar. 2023, doi: 10.1109/TTE.2022.3183171.

[18] R. Shahbazi and A. Rashidi, "Torque ripple reduction of switched reluctance motor by implementing a new converter based on DITC method," in *2023 IEEE Energy Conversion Congress and Exposition (ECCE)*, IEEE, Oct. 2023, pp. 5043–5048. doi: 10.1109/ECCE53617.2023.10362140.

[19] X. Guo, H. Deng, R. Zhong, and W. Hua, "Influence of torque sharing function parameters on torque ripple and online torque error compensation in switched reluctance machines," in *2022 25th International Conference on Electrical Machines and Systems (ICEMS)*, IEEE, Nov. 2022, pp. 1–6. doi: 10.1109/ICEMS56177.2022.9983206.

[20] L. Al Quraan, A. L. Saleh, and L. Szamel, "Indirect instantaneous torque control for switched reluctance motor based on improved torque sharing function," *IEEE Access*, vol. 12, pp. 11810–11821, 2024, doi: 10.1109/ACCESS.2024.3355389.

[21] G. Fang, J. Ye, D. Xiao, Z. Xia, and A. Emadi, "Computational-efficient model predictive torque control for switched reluctance machines with linear-model-based equivalent transformations," *IEEE Transactions on Industrial Electronics*, vol. 69, no. 6, pp. 5465–5477, Jun. 2022, doi: 10.1109/TIE.2021.3091918.

[22] Z. Omaç, "Fuzzy-logic-based robust speed control of switched reluctance motor for low and high speeds," *Turkish Journal of Electrical Engineering & Computer Sciences*, vol. 27, no. 1, pp. 316–329, Jan. 2019, doi: 10.3906/elk-1712-186.

[23] T. J. Ross, *Fuzzy logic with engineering applications*. Wiley, 2010.

[24] F. Ling, M. Ma, Q. Yang, and F. Li, "Torque ripple reduction of switched reluctance motor by segmented harmonic currents injection based on adaptive fuzzy logic control," in *2019 14th IEEE Conference on Industrial Electronics and Applications (ICIEA)*, IEEE, Jun. 2019, pp. 2429–2434. doi: 10.1109/ICIEA.2019.8834198.

[25] S. Kudiyarasan, N. Sthalasayanam, and V. Karunakaran, "Minimization of torque pulsations by using a novel fuzzy controller in SRM drives for EV applications," *Heliyon*, vol. 9, no. 3, p. e14437, Mar. 2023, doi: 10.1016/j.heliyon.2023.e14437.

BIOGRAPHIES OF AUTHORS

Rady Farouk Soliman was born in Giza, Egypt, in 1986. He received his B.Sc. degree in Electrical Power and Machines Engineering in 2010 and his M.Sc. in 2017 from Helwan University, Cairo, Egypt, where he is currently pursuing a Ph.D. His research interests include electric machine drives, machine control, switched reluctance motors, and permanent magnet induction generators. He can be contacted at email: rady.farouk@icloud.com.

Mahmoud Ramadan Ahmed was born in 1953 in Cairo, Egypt. He received his B.Sc. degree in Electrical Power and Machines Engineering in 1977 from Helwan University, his M.Sc. in 1981 from Cairo University, and his Ph.D. in 1987 from the University of Toronto, Canada. He served as a Research Associate at the University of Toronto from 1987 to 1990, and has been an Assistant Professor at Helwan University since 1992. His research areas include modeling and analysis of standalone wind energy systems, permanent magnet induction generators, and load assessment for renewable systems. He can be contacted at email: ramadan2153@gmail.com.

Soliman Mabrouk Sharaf was born in Minofia, Egypt, in 1949. He received his B.Sc. in Electrical Power and Machines Engineering in 1972 from Mataria, Helwan University; his M.Sc. in Power Electronics in 1979 from Helwan University; and his Ph.D. in 1985 from Queen's University of Belfast, United Kingdom. He has served in various academic positions at Helwan University, including Head of Department and Dean. From 2015 to 2018, he was Head of the Energy and Renewable Energy Department at the Egyptian Chinese University in Cairo. His research interests include power system control, electric machine engineering, wind and solar energy systems, and hybrid renewable power generation. He can be contacted at email: soliman_sharaf@yahoo.com.